



## Polylactic Acid /High-Ratio Natural Kenaf Fiber Biocomposite Sheets Processed by Calendering Melt Mixing Technique

M. Karevan\*

Department of Mechanical Engineering, Isfahan University of Technology, Isfahan, Iran

**ABSTRACT:** Biodegradable polymers reinforced with cellulose-based natural fibers are of high strategic necessities toward the environment preservation acts. Numerous studies have reported the formulation of polylactic acid based bio-degradable micro-composites loaded with natural fibers. However, the use of high natural filler content has been shown to be an underlying challenge in terms of bio-based composites' processability. This study mainly aims at the processability of thermoplastic bio-degradable composites of polylactic acid/Kenaf using a two-roller calendering machine on the melt mixing manner assisted with high shear forces. The results indicated successful processing of the green composites containing 0-30 wt% of kenaf using the sheet forming process from direct mixing of kenaf and polylactic acid granules. It was shown that the tensile modulus increased by 130% and the density of the parts decreased by ~10% at the filler loading of 30 wt% with respect to the neat polylactic acid whilst the tensile strength decreased irrespective of the filler loading. The results further showed the melting temperature decreases supporting better processability by increasing the kenaf fraction. The crystallization against the decrease in the density was correlated to the decrease in the toughness of the parts. Moreover, the morphology and structural studies whilst supporting the changes in mechanical performance supported the effect of processing on the fillers orientation and the possible presence of agglomerated phase at higher filler loadings.

### Review History:

Received: Oct. 03, 2021

Revised: Jan. 03, 2022

Accepted: Feb. 05, 2022

Available Online: Feb. 11, 2022

### Keywords:

Calendering

Polylactic acid

Kenaf fiber

Two-roller mixer

Micro-composites

### 1- Introduction

Besides many other applications, green bio-degradable composites whose components are usually extracted from natural resources are used in packaging industries as well as the development of green technologies such as structure sectors, automotive industries, or even fields such as bio-and tissue engineering [1, 2]. The scission of polymer chains due to microbial attack through enzymatic actions of microorganisms leading to hydrolysis results in degradation and decomposition of bio-degradable composites. This generation of green materials is able to be recycled when made of bio-degradable polymers or be applied as a surface coating in the design and fabrication of automotive body parts with bio-degradable properties in the form of sheets or thin films. The main challenge is the persistence of petroleum-based polymers, lack of landfills, and shortage of petroleum resources, and further extended to destroying the environment and animals' life. Moreover, growing awareness of global environmental factors integrated with a sustainable economy, ecoefficiency, and the need for green engineering and thus products have spurred motivation for the use of advanced technologies and emerging bio-based materials compatible

with the environment. This impetus has urged a significant body of studies reported elsewhere in the literature [3, 4].

Biofibers together with biodegradable polymers have been introduced as a replacement for non-recyclable and non-renewable polymers that in many aspects could be competitive with synthetic traditional composites. Although natural fibers including jute, sisal, kenaf, and hemp may offer lower strength and modulus compared to glass or metallic fibers, the goal is mainly the development of bio-degradable sheets where mechanical strength is of lower importance with respect to their applications [5, 6]. On the other hand, petroleum-based polymers as traditional ones such as polypropylene, polyethylene, polyester, and epoxy have been largely used in the development of composites. However, today's applications such as those in packaging and farming call for bio-degradable polymers [7, 8]. In terms of costs and accessibility, substitutes for bio-degradable polymers should be taken into consideration. One main factor leading to the high cost of biodegradable composites is the processing technique itself. Wide applications and demand for such green composites thus have urged novel processing methods for their extended volume production. Even though the main purpose of developing composites is to improve their mechanical and physical properties such as stiffness, and processability, the introduction of more advanced techniques thus needs

\*Corresponding author's email: mkarevan@iut.ac.ir



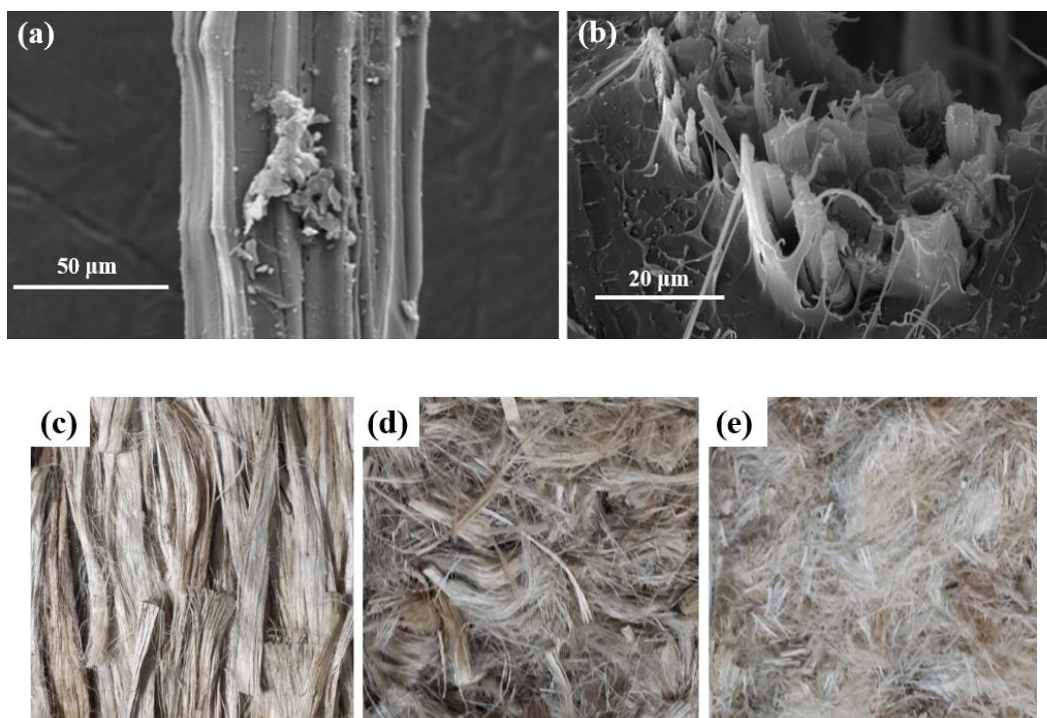


**Fig. 1. (a) Representative Scanning Electron Microscope (SEM) image of kenaf fiber, (b) embedded single fiber cross-sectional fracture within PLA polymer matrix, and (c-e) as-received and chopped kenaf fibers before the melt mixing process**

further investigation toward the fabrication of sheets or thin films with biodegradable properties. Bio-polymers including Polylactic Acid (PLA), cellulose esters, soy-based plastic, starch plastic, xanthan, or those derived from vegetable oils and bio-based resins, etc. have been extensively employed for the fabrication of green composites [9-11]. Although extensive studies have been reported on the effect of various natural fillers on the mechanical properties of PLA reinforced composites, most of the research has incorporated bulk fabrication of the parts per specific standards that may not be necessarily representative of end-use products due to the different geometry and shape besides the size effect differences in terms of performance [6, 9, 12, 13]. Another main challenge in the fabrication of bio-based composites is the lack of enough wettability of polymers when traditional techniques such as extrusion injection molding are used due mainly to the increased viscosity of the melted compound or less fluidity of polymer melt within the mold due to the absence of shear forces in the case of hot press technique [13, 14]. This unfavorable effect is even more intensified when high natural filler weight fractions are to be used. The latter will result in poor interfacial interaction and adhesion leading to imperfect load transfer from the matrix to the fiber and thus low mechanical performance [15-19].

The main focus of this work is examining the feasibility of two roller mixer calendering as a high shear melt mixing process in the fabrication of bio-degradable thermoplastic sheets supported by the overall mechanical and thermal response of the fabricated parts. This research, therefore,

incorporates the fabrication of PLA micro-composites sheets with kenaf fiber as the reinforcing phase to assess the feasibility of a two-roller mixer in regard to the enhancement of PLA wetting ability at the interface of fibers following the dispersion/distribution level of the filers linked with tensile and thermal properties of the fabricated sheets. It is hypothesized the high shear forces applied by the rolls through the composite melt coupled with the thermal experience exposed by heating rolls around the melt temperature of the compounds result in the fabrication of uniform homogenous sheets of enhanced stiffness. The changes in the crystallization and morphology of the fabricated parts were then used to better understand the mechanical performance of the sheets against the changes in kenaf fiber. The current study may be considered a breakthrough in the development of thin sheet green composites based on melt mixing utilizing calendering technique whilst the interrelation amongst mechanical, thermal, and structural behavior of the specimens are highlighted to give better insight toward the feasibility of the process.

## 2- Experimental

### 2- 1- Materials

For the fabrication of the bio-degradable composites, PLA granules produced by KAS Gmbh (Australia) were used as the bio-based matrix material. Natural kenaf fiber (imported from Malaysia) with a diameter as represented in Fig. 1 was purchased from a local supplier. The figure shows a representative morphology and geometry of the fibers

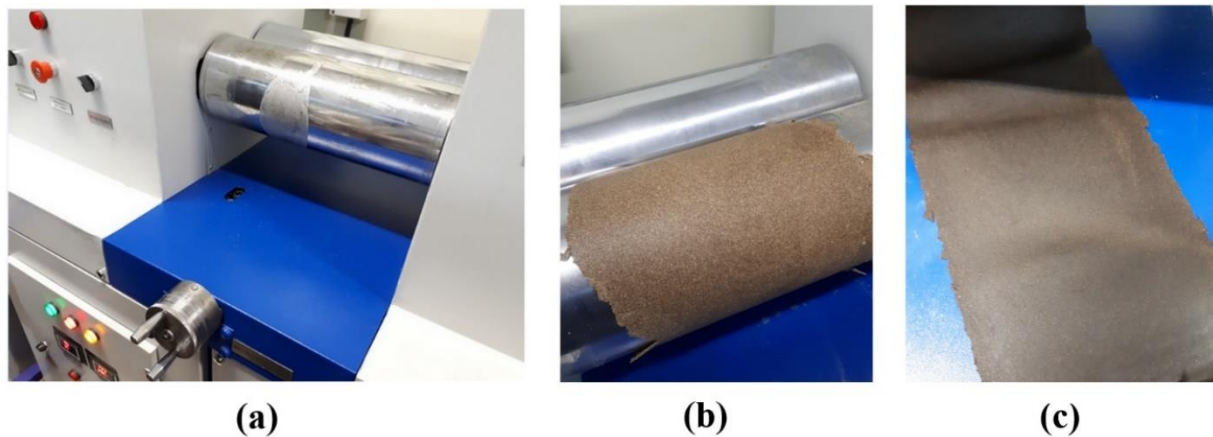


**Fig. 2. Sheet processing of cellulose based PLA composites using two rollers calendering machine: (a) the roller device, (b) composite compound melt rolled within the gap between two rotating heated rolls under high shear forces, and (c) a representative bio-based PLA composite after removal from rolls. (Photo courtesy of the Polymer and Nanocomposites Lab, Isfahan University of Technology, Isfahan, Iran)**

used in this research [20]. The fractured surface of a single kenaf fiber embedded within the PLA matrix upon a brittle impact test is represented in Fig. 1(b) demonstrating the fibril structure of the fiber. Figs. 1 (c-e) depict the actual shape of the kenaf used in the melt mixing process before and after being chopped with no use of surface chemical modification.

## 2- 2- Fabrication of bio-degradable Kenaf/PLA composites

As received kenaf with no further functionalization and chemical treatment was used as the bio-based filler. However, to ensure the removal of moisture present in the fibers, the kenaf fillers were vacuum dried within a vacuum oven at 80 °C for 1 hr. The fibers then were chopped into ~ 2-3 mm length above the critical length of fibers estimated in our previous work reported in [21]. It is noted that the critical length of fibers plays a key role in the interfacial load transfer at the interface of filler/polymer and the length depends on the quality of the interfacial surface, the tensile strength, and the aspect ratio of the fiber [22]. The bio-degradable composite sheets of PLA reinforced with 0 to 30 wt% (weight fraction in percent) of kenaf were fabricated with direct melt blending of kenaf fibers and PLA using a calendering machine under the simultaneous presence of heat and shear forces with rollers temperature of ~ 150 °C at 5-10 rpm. To ensure enhanced dispersion/distribution of the kenaf fiber within the PLA melt, the process was continued for 30 minutes. Based on the process specific ability to implement high shear forces on the kenaf/PLA blend, the process proved to be successful in complete wetting of the kenaf surface by the PLA melt even at higher kenaf loadings. The processing window of the fabrication stage followed the melting behavior of the composites upon the thermal analysis performed as reported in the next part.

Finally, the fabricated kenaf/PLA sheets were removed from the surface of rollers after the compound solidification during an air cool condition after around 45 minutes when the rolls' temperature reached the glass transition temperature of the composite compound. Fig. 2 represents the calendering set-up and processing in the fabrication of the specimens in this study. The roller device used in the fabrication of kenaf/PLA sheets with the nominal power of 1500 watt, 5-60 rpm, rolls length/diameter of 40/15, and gap of 0-5 mm is depicted in Fig. 2(a). The processing of bio-based sheets of PLA during the calendering process and the final sheet specimen followed by air cooling of the thermoplastic composite sheet of cellulose based PLA on the two-roller calendering are shown in Fig. 2(b) and (c), respectively. As clearly seen from the figure, successful fabrication of homogenous high-ratio content reinforced sheets of uniform thickness is exhibited.

## 2- 3- Characterization of kenaf/PLA composites

### 2- 3- 1- Tensile properties of kenaf/PLA composites

Mechanical behavior including the tensile modulus, tensile strength, and strain at break of the PLA reinforced with kenaf fiber was evaluated according to the ASTM D882 test method using a universal tensile testing machine (Sanaf Co., Iran). The specimens in the form of composite strips were cut measuring 120×12 mm<sup>2</sup> and a thickness below 1 mm (an average of 500 μm). It is noted that due to the free contraction of polymeric sheets in the air after the calendering process, unlike other fabrication processes as seen in the case of extrusion-injection molding as well as limitations in the resolution of the displacing ruler (used to adjust the gap distance), the thickness of the fabricated composites varied around the said average value as reported. Three tensile test specimens were cut from each composite sheet at least

an average of two specimens were reported. Measurements were obtained at the deformation rate of 2.54 mm/min at the ambient temperature. It is noted that to calculate the modulus, the very initial points on the stress-strain curves were discarded due to the possibility of initial non-uniform tension in specimens. Then data points in the very linear region were selected and data fitted using a software linear function. The slope was recorded as the tensile modulus.

### 2- 3- 2- Thermal behavior of the composites

The thermal properties of the composites including melting temperature, the heat of enthalpy, crystallization behavior, and the glass transition temperature ( $T_g$ ) were assessed using the Differential Scanning Calorimetry (DSC) method on DSC equipment (Sanaf Co., Iran) per the ASTM D3418. The thermal analysis was conducted utilizing the temperature ramp from the ambient to 200°C with the heating rate of 10°C/min under the constant flow rate of dry nitrogen. The samples measured around 10-20 mgr for each test. The crystallinity of the kenaf/PLA composites,  $X_c$ , was estimated using Eq. (1) as follows:

$$X_c (\%) = \frac{H_m}{[H_0(1-wt\%)]} \times 100 \quad (1)$$

where  $H_m$  is the heat of fusion (melt/or solidification enthalpy) obtained from the DSC trace during the endothermic transition, wt% is the filler content in weight fraction,  $H_0$  is the enthalpy of melting of the fully crystalline PLA taken ~ 93.7 J/gr [23].

### 2- 3- 3- Morphology of the composites

The morphology of the fractured surface of the samples including the quality of kenaf dispersion and distribution within the PLA phase were examined utilizing the Scanning Electron Microscope (SEM) technique using FE-SEM QUANTA FEG 450 (USA). The fractured surface of the kenaf/PLA composites was gold sputtered before the SEM analysis to avoid charging effects on the non-conductive surface of the samples.

### 2- 3- 4- Microstructure and crystals analysis

X-Ray Diffraction (XRD) technique was performed to identify the structure of the PLA biocomposites reinforced with kenaf fibers and the crystallization characteristics of the composites. The XRD analysis was employed using XRD equipment with a Cu K $\alpha$  radiation source ( $\lambda = 1.5418 \text{ \AA}$ ) generating X-rays. The bio-composite specimens were scanned in the  $2\theta$  range from 5° to 70° with a 0.02° step size. The X-ray equipment was operated at 40 kV and 30 mA. The XRD spectra, peak location, and peaks intensity were used for the estimation of the lamella thickness of crystals according to the Debye-Scherrer's formula as expressed by Eq. (2) and the full width at half maximum of the predominant characteristic peak diffractions observed through the XRD patterns within the  $2\theta$  range.

$$L_t = \frac{k \lambda}{\beta \cos \theta} \quad (2)$$

where  $L_t$  is the lamella thickness,  $K$  is the crystal shape factor taken as 0.9,  $\lambda$  is the wavelength of the X-ray radiation (0.154 nm),  $\beta$  is the full width at half maximum, and  $\theta$  is the peak position of the XRD pattern diffractions as the crystallites characteristic peak.

### 2- 3- 5- Density measurement

To assess the stiffness of the specimens and understand the correlation between the structure and overall tensile response upon the addition of kenaf fiber, the relative density of the fabricated kenaf/PLA parts was evaluated using a 4-digit densitometer on the bases of the Archimedes' method. The density of at least three samples cut from the composite sheets from the entire thickness was characterized and the average value was reported. The density of neat kenaf fibers was also measured for the sake of comparison. To ensure the absence of artificial errors due to the presence of bubbles and air gap between the specimens and the immersed tray, the surface of the specimens was thoroughly wetted before the experiments.

## 3- Results and Discussion

### 3- 1- Tensile properties of kenaf/PLA composites

The stress-strain curves of the kenaf/PLA composites fabricated are shown in Fig. 1. As understood, the addition of kenaf resulted in a decrease in the tensile strength of the specimens. The findings could be associated with the imperfect bonding at the interface of kenaf/PLA at rather high filler ratios of 10-30 wt%. This occurs mainly due to the lower ability of the polymer to perfectly wet the surface of the kenaf. Moreover, it should be noted that as mentioned earlier the kenaf used in this experiment did not experience any functionalization and was used as received. A key factor in the presence of the lower load transfer at the interface could be ascribed to the rather hydrophobic nature of the PLA as reportedly around 70° to 85° with respect to that of the surface kenaf fiber being more hydrophilic being ~ 55° [24-26]. This difference may be another reason supporting the dropped tensile strength of the composites with the addition of kenaf. The results further exhibited that with the addition of kenaf wt% the strain at break and thus the toughness of the specimens decreased. However, it is believed that considering the actual application of the PLA based composites in packaging industries and kenaf as an inexpensive replacement for PLA, the decrease in tensile properties needs to be justified and in case of the need for better improvement of the composites, surface treatment, and fiber surface fictionalization with use of NaOH or other alkaline treatment should be conducted [20].

Fig. 4 illustrates the tensile modulus and tensile strength of the kenaf/PLA composites in Figs. 4(a) and (b), respectively, summarizes the finding reported in Fig. 3. It can be understood from Fig. 4(a) that unlike the changes in the

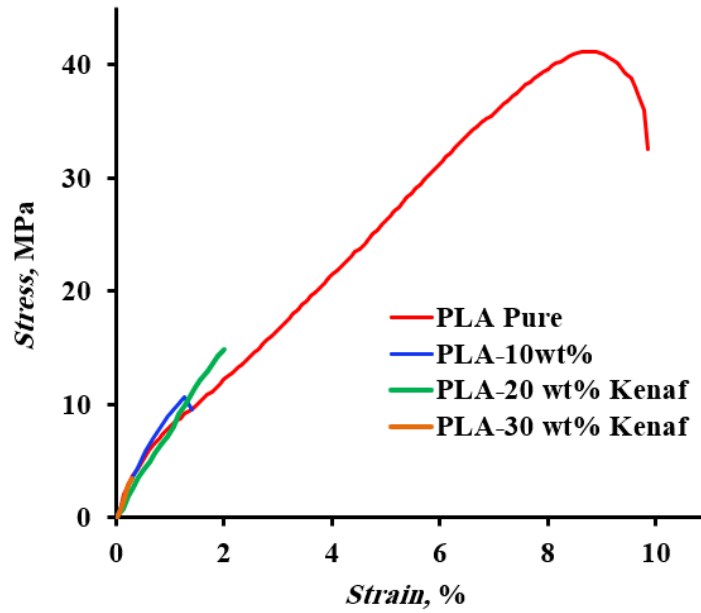


Fig. 3. Representative stress-strain curve of the PLA composites reinforced with 0-30 wt% of kenaf

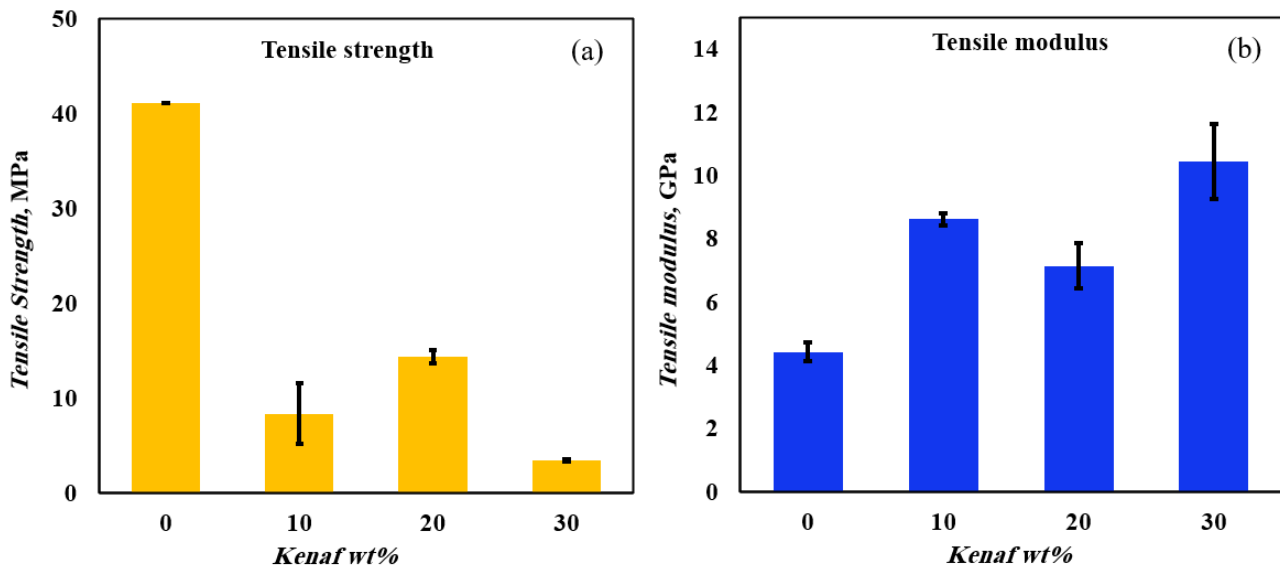


Fig. 4. (a) Tensile modulus and (b) tensile strength of the PLA reinforced with kenaf fiber v.s. the filler content

tensile strength as depicted in Fig. 4(b), the tensile modulus of the composites increases upon the addition of kenaf. This expected result further confirms the rule of mixtures where the addition of high modulus fiber modifies the properties of composites. Considering the decrease in the density of the parts against the addition of filler as shown in the next parts, the ratio of modulus to weight is further increased as

a desirable property in structural designs. It is noted that the tensile strength is much more sensitive to the hydrophobic nature of PLA which may contribute to the formation of imperfect interfacial sites and micro-bubbles around the filler [22]. The findings will be discussed in the next part when the crystallization behavior of the specimens needs to be more tightly related to the observed mechanical properties. The

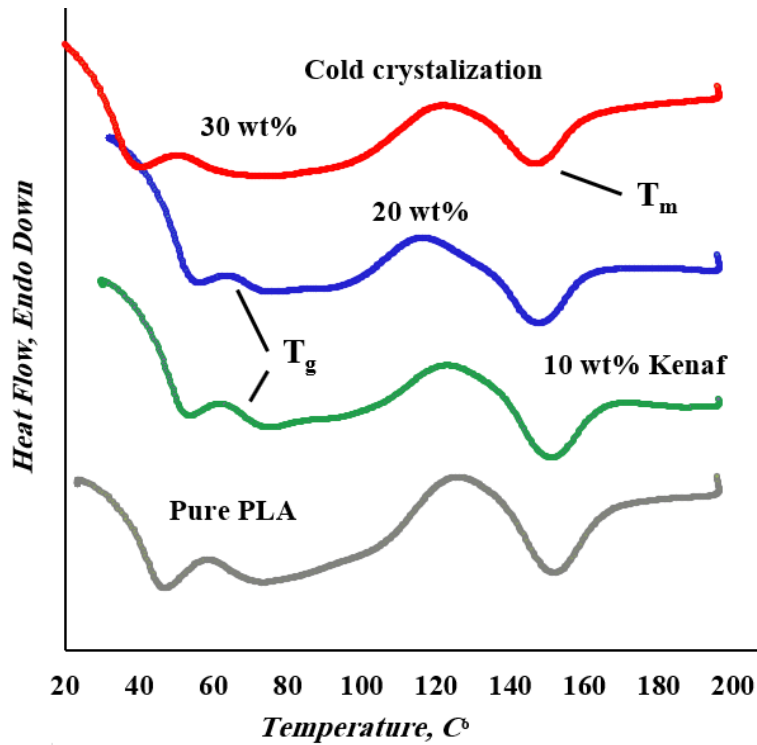


Fig. 5. DSC thermograms of the kenaf/ PLA composites in the heating scan as a function of the kenaf wt%

Table 1. Thermal and crystallization properties of the kenaf PLA composites in the heating scan as a function of the kenaf wt%

Sample	$T_g$ °C	$T_m$ Onset °C	$T_m$ Final °C	$T_m$ °C	$\Delta H$ J/gr	X%
Pure PLA	66.3	127.0	171.0	152.4	25.5	27.2
10wt%Kenaf	70.0	124.7	169.0	152.2	21.2	25.2
20wt%Kenaf	70.0	118.7	167.7	148.5	21.6	28.8
30wt%Kenaf	58.1	123.4	167.9	147.6	17.9	27.3

broad standard deviation about the average in the case of 30 wt% reinforced PLA can be attributed to the inhomogeneous texture of the PLA composite sheets due to the non-uniform distribution of high filler content within the matrix. It is noteworthy to mention that higher degrees of kenaf wt% adversely influence the wetting ability of polymer and possible crystal nucleating sites due to a lack of enough interfacial polymer [11, 27, 28].

### 3- 2- Thermal behavior of kenaf/PLA bio-composites

Fig. 5. represents the DSC thermograms over the heating scan of the kenaf/PLA composites. As seen, two underlying transition zones as endothermic phase transformation are observed. It is shown that upon the heating scan all composite systems exhibit the  $T_g$  and melting point at their expected temperatures. The results have been summarized in Table 1. It is noted that a rather large exothermic peak appears in the

case of all composites associated with the cold crystallization behavior of the composites before the enthalpy zone of melting near the onset of melting at around 118 to 124 °C. The imperfect crystallization behavior of the specimens is responsible for the cold crystallization and is correlated to the cooling conditions of the polymer and composites after the calendaring process [29, 30].

It is hypothesized that due to air cool conditions and, thus, the rapid cooling during the solidification, the polymer phase would be in shortage of time to be transformed into crystalline lamella. This phenomenon is suggested to be more serious in the case of pure PLA due to its possible higher thermal conductivity than the reinforced composites. On the other hand, in the case of kenaf reinforced PLA the enthalpy of the cold crystallization decreases with the addition of kenaf wt%. This finding can be explained by the fact that when the filler is incorporated into the PLA matrix, the lower rate of heat transfer impedes sudden cooling conditions which will contribute to the development of higher degrees of crystallization, greater thickness of lamella, and, thus, the existence of more perfect crystals when the kenaf content grows compared to the case of the neat PLA. However, it should be noted that there exist several factors competing against the formation of crystals in reinforced composites. For instance, with the addition of fillers, the reinforcement phase acts as impeding sites that interfere with the crystals' growth as the crystalline spherulites impinge on one another during the formation. Furthermore, at higher filler loadings, the possibility of agglomerated phase is inevitable. The latter leads to a decrease in the available surface of fillers as acting sites for the formation of crystals. The factors mentioned could adversely or synergistically contribute to the overall crystallization behavior of semi-crystalline polymer composites [27, 31, 32].

Table 1 represents the summary of the results obtained from the DSC analysis. As understood, there is an initial increase in the  $T_g$  of the composites followed by a decrease in the  $T_g$  value. The findings are attributed to the developed interfacial interactions at the interface of kenaf/PLA that impede the free movement of polymer chains contributing to the increase in the  $T_g$ . However, upon the addition of greater kenaf content, the agglomeration of filler and lower degrees of the wetted surface of kenaf only partially influence the polymer chain mobilization and thus the decrease in the  $T_g$  [33-35].

The DSC results also confirm the highest degree of crystallization in the case of 20 wt% kenaf. However, it can be understood that the addition of fillers acted like nucleating agents leading to the formation of crystallites. The greater value of crystallization in the case of pure polymer is related to the pinning effect of the filler against the nucleation ability provided in the formation of spherulites [36]. These compromising effects explain variations in the modulus and the decrease observed in the tensile strength of the kenaf/PLA specimens fabricated. As shown in Table 1, an overall decrease in the melting temperature is observed that is correlated to the thinner lamella thickness generated during the fabrication

process. This observation could be well explained by the impeding effect of kenaf against the crystallite growth and thus the presence of the thinner crystals [32]. The results could be further supported by the XRD analysis as described in the next parts.

### 3- 3- Specific density

One of the key goals of the current research was the development of kenaf-based bio-composites of high stiffness. One needs to keep in mind that the stiffness of a part incorporates two simultaneous factors; one goes for the mechanical response such as the modulus and the second the lightness of the part. As shown in Fig. 6, the specific density with the addition of kenaf decreases, which in turn contributed to the stiffness of the parts. The specific density values have been summarized in Table 2. Considering the enhanced modulus of the composites systems with increasing the filler content, it could be easily shown the ratio of the modulus to the weight of specimens obviously increase with filler content. The results confirm that the kenaf has a favorable effect on the stiffness of the part fabricated by the calendaring process in this work. It should be noted that a portion of the decrease in the density might be stemmed from the imperfect bonding and suppressed wettability of polymer at high kenaf content. Whilst this undesired effect led to the decrease in the tensile performance of the parts, in terms of the modulus this lowered density assists in the increase in the stiffness of the parts.

Through a simple calculation one may understand that by the consideration of the stiffness definition, the addition of kenaf fiber up to 30 wt% will increase the modulus to density ratio by around 200% with respect to that of neat PLA.

### 3- 4- XRD micro-structural analysis of kenaf/PLA specimens

XRD experiments were conducted to give better insight into the correlations amongst the microstructure and eventual mechanical and thermal response of the fabricated bio-composites against the increase in the PLA content. Fig. 7 represents the XRD pattern of the kenaf/PLA composite sheets processed by the calendaring device as the melt mixing step in this study. The XRD characteristic values of the melt mixed parts are summarized in Table 3. The findings confirm that there exists no predominant crystallization characteristic peak in the case of neat PLA sheets whilst the dominant amorphous region of the PLA is observable by an amorphous halo as frequently reported in the case of PLA based biocomposites [37]. This broad amorphous hill is exhibited by all composite systems irrespective of the filler loading used and ranges from  $\sim 10^\circ$  to  $25^\circ$  as shown through the XRD patterns. The absence of any crystallization peak associated with the PLA phase suggests the PLA chains have been incompletely ordered and packed resulting in a rather low degree of crystallization correlated to the PLA region as earlier shown by the DSC analysis represented in Table 1.

The lower crystallinity of the specimens could be ascribed to the high cooling rate of the reinforced polymer melt during the calendaring process where, unlike in the case of

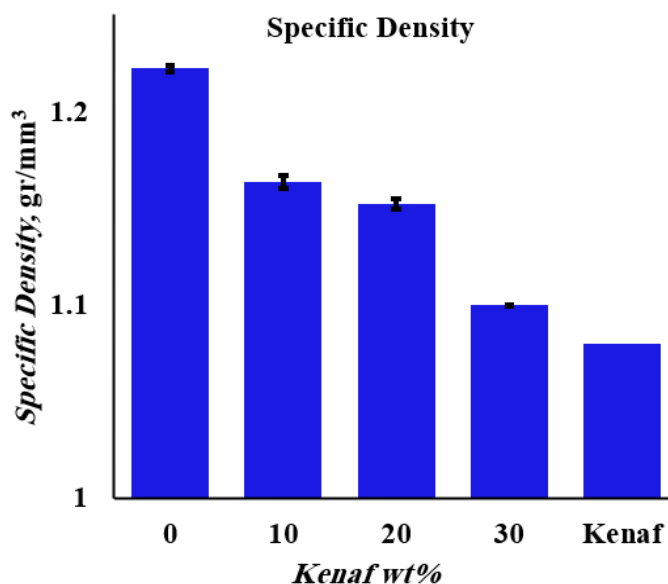


Fig. 6. Specific density of the kenaf/PLA specimens with the addition of kenaf content

Table 2. Specific density values of the fabricated kenaf/PLA sheets

Sample	Density $\frac{\text{gr}}{\text{mm}^3}$
Pure PLA	1.22±0.001
10wt%Kenaf	1.16±0.003
20wt%Kenaf	1.15±0.003
30wt%Kenaf	1.10±0.0001
Pure Kenaf fiber	1.08

injection molded parts, the melt exposure to air expedites the solidification of the sheets leading to amorphous chains with less time available to be accommodated as orderly packed phases so far called the crystalline region. Fig. 7 further demonstrates the appearance of kenaf fiber characteristic peaks forming on the halo amorphous peak of PLA around two separate  $2\theta$  angles of  $\sim 15^\circ$  and  $22^\circ$ . As clearly shown, these characteristic peaks are markedly intensified with the addition of greater kenaf loading as reported also in Table 3. As reported elsewhere, the peak is associated with the cellulose I $\beta$  phase within the kenaf structure [31]. As understood from Table 3, no changes in the d-spacing of kenaf predominant crystals nor the creation of other types of

crystals are observed when the sheets have experienced the calendaring process under severe shear stresses.

It should be mentioned that the kenaf fibers used in the current research have not experienced any chemical modification. So, it is expected that the kenaf fibers consist of hemicellulose and lignin as amorphous polymers resulting in no changes in the crystallization of the fibers upon calendaring melt mixing process as expected. It is further shown by Fig. 7 and the characteristic parameters reported in Table 3 that upon the addition of kenaf from 10 wt% to 20 wt%, a decrease in the intensity peak associated with the first and second  $2\theta$  angles occurs. This finding supports better dispersion of the kenaf phase in the case of 20 wt%

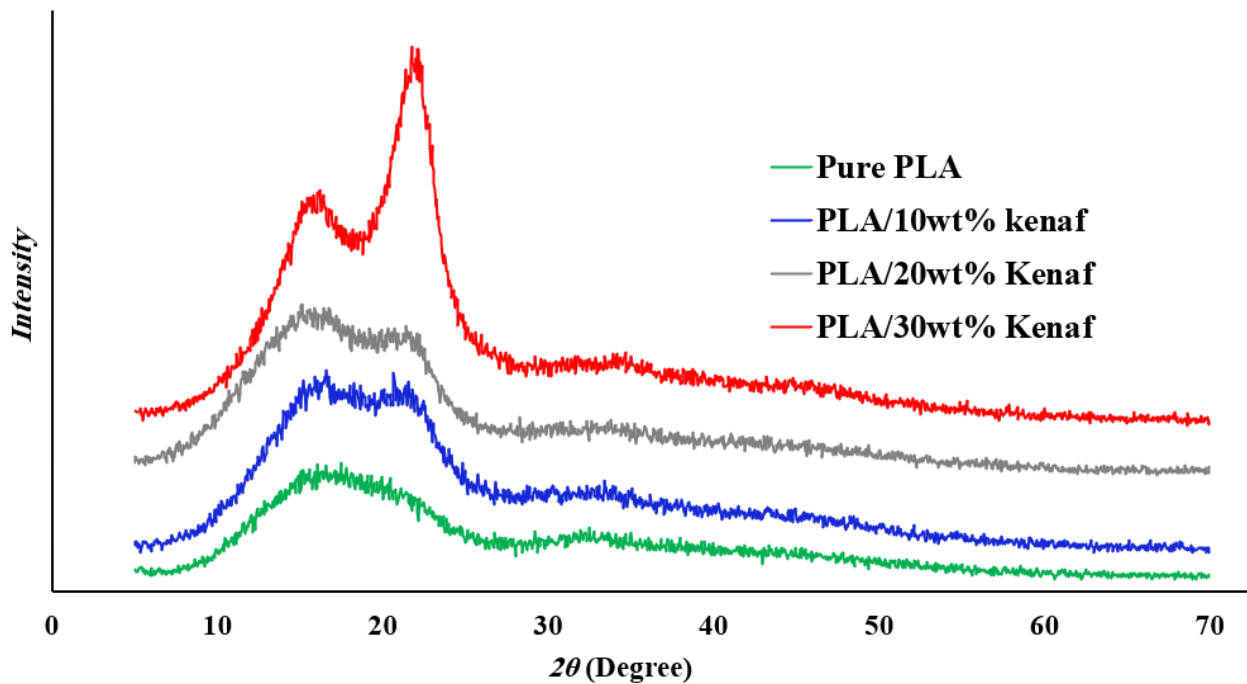
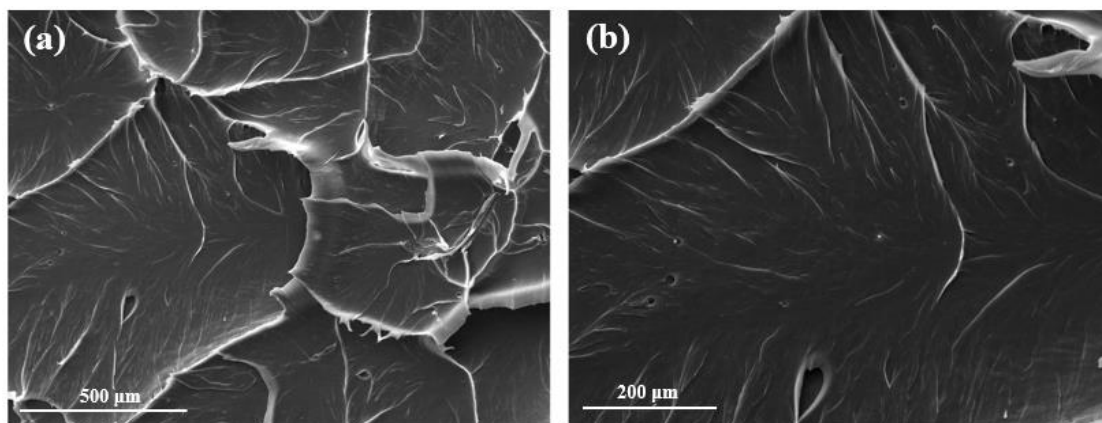


Fig. 7. XRD patterns of pure PLA and Kenaf/PLA bio-composites

Table 3. XRD characteristic  $2\theta$  angles and crystallinity index of composite components exhibiting by the pure PLA and kenaf/PLA filled with 10 to 30 wt% of kenaf fibers

Sample	PLA				Kenaf			
	First peak		Second peak		First peak		Second peak	
	$2\theta^a$	$P.I^b$ (a.u)	$2\theta$ ( $^\circ$ ) <sup>a</sup>	$P.I^b$ (a.u)	$2\theta^a$	$P.I^b$ (a.u)	$2\theta^a$	$P.I^b$ (a.u)
Pure PLA	16.7	295.2	32.5	35.4	-	-	-	-
10wt%Kenaf	-	-	33.6	33.7	15.8	467.2	22.1	373.9
20wt%Kenaf	-	-	33.3	37.0	15.7	464.7	21.8	350.8
30wt%Kenaf	-	-	34.1	173.6	15.7	657.1	22.1	1093.1

<sup>a</sup> 2-theta (degree) <sup>b</sup> Peak intensity



**Fig. 8. SEM micrographs of neat PLA composites fractured surface at different magnifications**

kenaf content. The latter is explained by the fact that with the addition of rigid fillers, the melt viscosity of the compound existing within the calendaring rolls increases which leads to the increase in the shear forces applied to the polymer melt [28, 32]. This effect in turn will contribute to the destruction of agglomerated phase as confirmed by the SEM images as explained later in this work. Moreover, upon the addition of kenaf fibers, the specimens lead to a greater degree of filler alignment, which, in turn, results in lower peak intensity. However, with further increase of the kenaf content, the presence of a severe agglomeration phase is inevitable as later shown via the SEM results. The effect of kenaf bundles or entangled phase could be, thus, interrelated to the increase in the crystallization followed by the decrease in the degree of crystallinity as the filler content increases as shown in Table 1. The changes in the crystallization could be thus correlated to the kenaf surface available for the polymer chains as a nucleating site for crystallite formation. Above this, as a deteriorating secondary effect, a high degree of kenaf fibers impose unfavorable pinning sites that constrain the crystal formation. The finding is in good agreement with the unchanged melt temperature of the specimens upon addition of kenaf at higher filler loading as understood from Table 1 and Fig. 5. As the secondary mechanism, the interphase region can act a reinforcing factor contributing to the elastic response of composites.

As reported frequently, the presence of the agglomerated phase results in suppressed interfacial filler/polymer interactions and thus the formation lower amount of rigid interphase [38-40]. The latter could be a reason for the decrease in the overall elastic response of the fabricated specimens at higher kenaf loadings. The finding is in good agreement with the decrease in the  $T_g$  of the bio-composites when the sheets are reinforced with rather high filler content as understood from Table 1.

### 3- 5- Morphology of the kenaf/PLA bio-composites

The SEM photomicrographs of pure PLA fractured surface perpendicular to the calendaring tangential shearing force direction are represented in Fig. 8. It is clearly understood that a majority of the surface involves a smooth brittle fracture nature as attributed to the nature of PLA as a brittle bio-based polymer. Fig. 9 depicts the SEM micrographs of the kenaf/PLA composites fractured surface filled with 10 wt% of kenaf representing different magnifications. The fiber region is clearly shown in the figure exhibiting rather random orientation of the kenaf fibers within the matrix. Moreover, it is clearly shown that no filler pull-out exists upon applying impact load confirming strong interfacial bonding at the interface of kenaf and PLA whilst longitudinal breakage of fibers appears upon the fracture. In addition, it could be represented that no or few agglomerated sites are present, which is mainly ascribed to the low kenaf content of 10wt% and, thus, enhanced wettability of polymer melt during the melt mixing step as the calendaring process is performed. It is noted that the finding is in good agreement with other structural analyses performed in the study. First, the XRD curves show a rather flat characteristic peak in the case of 10 wt% filled composites exhibiting a minimal presence of agglomerated phase. Second, the DSC results exhibit the improved glass transition of the 10 wt% kenaf/PLA composites with respect to other cases. As the  $T_g$  is linked to the immobilization of the amorphous phase as a result of interfacial interactions, the enhanced  $T_g$  value could be thought of effective available surface of the kenaf phase.

It is further confirmed by Figs. 9(b) and (c) that there exist only a few interfacial voids and detachment sites at the interface of fibers and PLA suggesting the forced adhesion of interfacial kenaf and PLA surface resulting from the compressive forces applied onto the polymer compound existing between the rolls during the calendaring process.

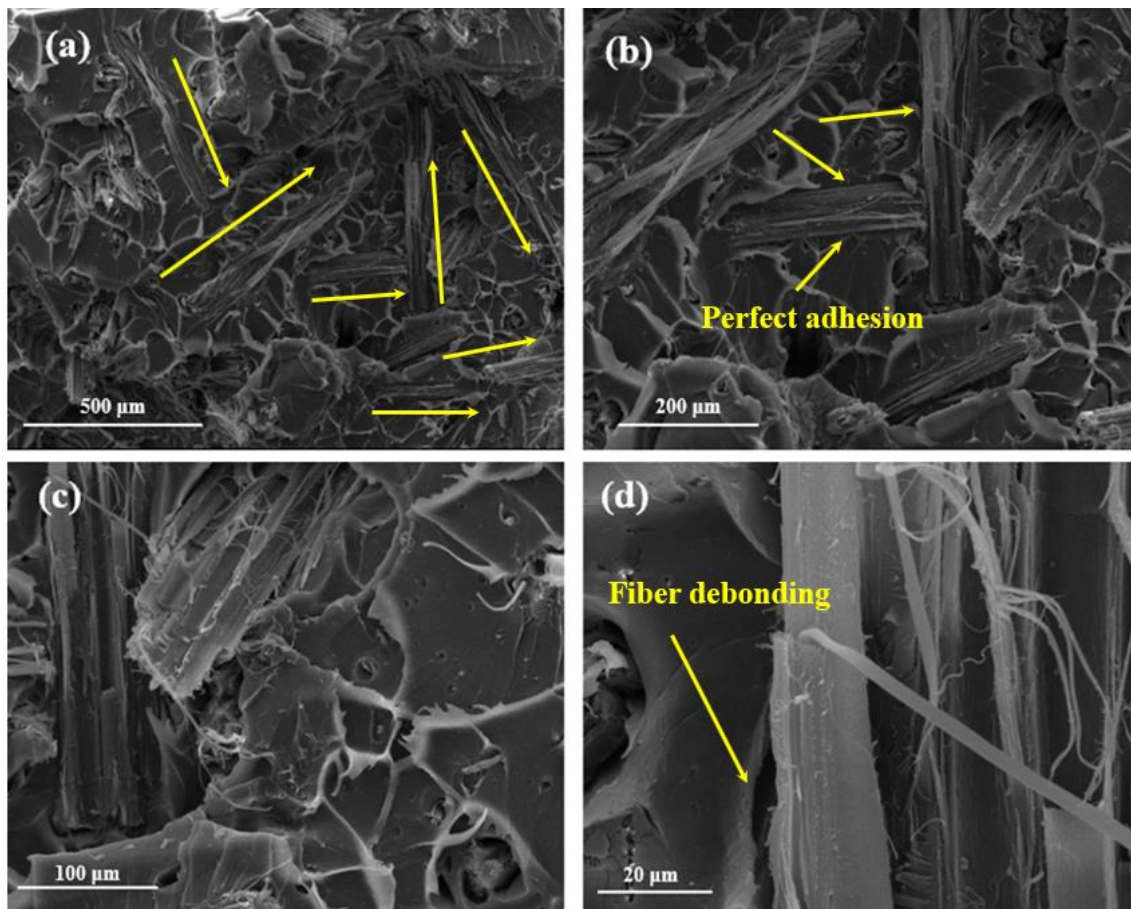


**Fig. 9. SEM micrographs of the kenaf/PLA composites fractured surface reinforced with 10 wt% of kenaf content at different magnifications**

The figure further represents that there is minimal or no fiber pull-out out of the matrix, which is widely accepted as the main evidence of poor filler/polymer bonding. The SEM observations confirmed that even with the addition of higher kenaf loading, a strong interfacial bonding exists within the parts as shown later in this work. It is also noted that as the fiber pull-out mechanism is mainly responsible for energy consumption [41], the results support the decrease in the overall elastic response of the kenaf reinforced bio-composites with respect to the neat PLA. The findings thus demonstrate that the kenaf fibers do not participate in bearing load transfer from the PLA align the fibers. This could be better explained by the random orientation of the fillers when the effective aspect ratio of the fibers has decreased when the tensile load is not perfectly aligned with the direction of embedded fibers [42].

The zoomed-in micrograph as illustrated in Fig. 9(d)

shows the presence of kenaf fibrils upon the fracture. Fig. 10 displays the fractured surface of PLA bio-composites filed with higher filler ratios of 20wt% (Figs. 10(a) and (b)) and 30wt% (Fig. 10(c) and (d)). Whilst the perfect interfacial bonding still is observable at the filler/matrix, unlike the case of bio-composites filled with 10wt% of kenaf as described earlier, rather unidirectionally aligned kenaf fibers are present over the fractured surface in the case of 20 and 30wt% bio-composites as expressed in Figs. 10(a) and (c). The findings confirm an enhanced shear tangential shear forces applied within the rolls' gap, which is ascribed to increased viscosity of the compound melt when greater fractions of kenaf have been incorporated into the PLA [32].

The results revealed could support the improvement in tensile strength of 20 wt% PLA/composites as earlier reported in Fig. 4(b). Fig. 10(c) shows the presence of more sites rich in kenaf fibers compared to specimens filled with 20wt% of

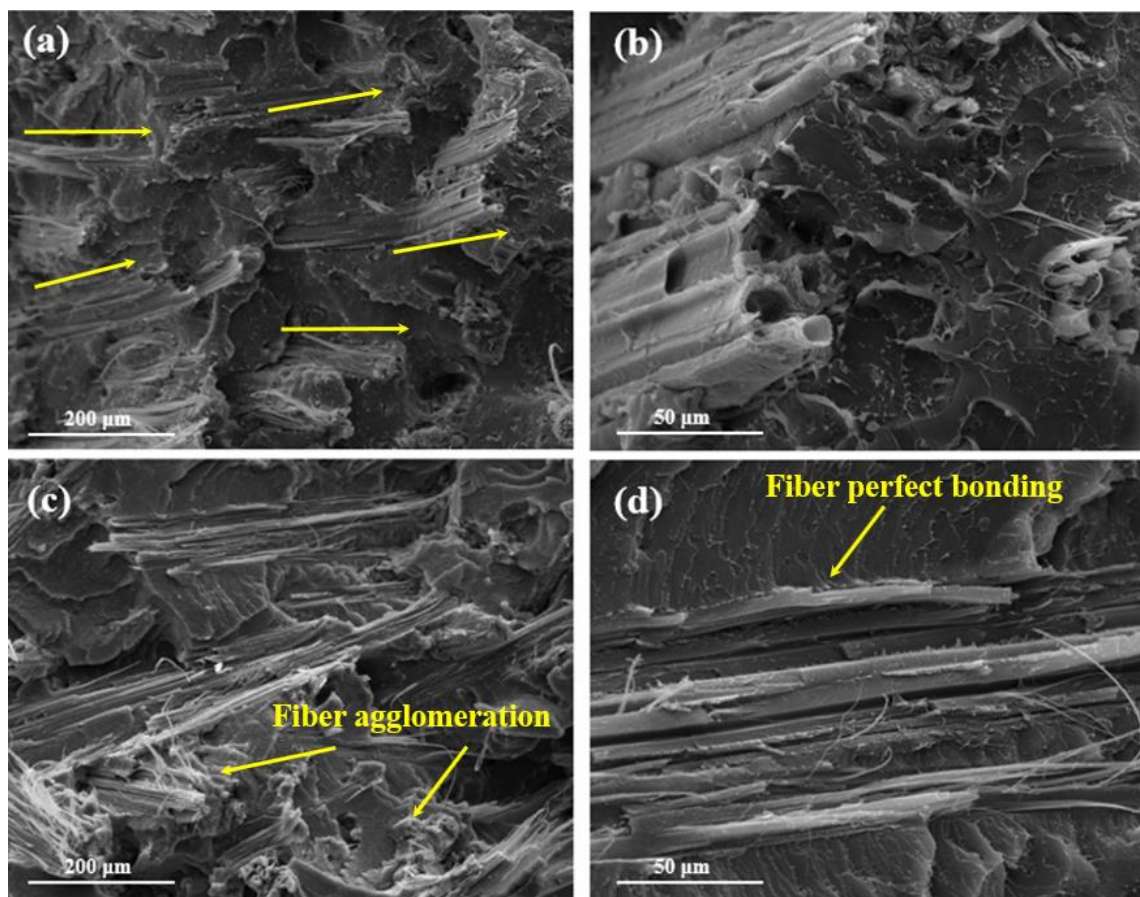


**Fig. 10. SEM micrographs of the kenaf/PLA composites fractured surface reinforced with (a, b) 20 wt% and (c, d) 30 wt% of kenaf content at different magnifications**

fibers as expected. Although the adhesion at the interface of a fraction of fibers is clearly exhibited (Fig. 10(d)), the presence of agglomerated fibers with the lowered wetted surface is shown in the figure. The latter could explain the decrease in the tensile response of the fabricated sheets upon the addition of kenaf beyond 20wt% [43].

#### 4- Conclusion

The feasibility of the melt mixing technique on a two-roller calendering device for the fabrication of kenaf fiber reinforced PLA based bio-composites was examined. Kenaf/PLA composite sheets reinforced with a rather high ratio kenaf content of 0-30 wt% were prepared to take the advantage of assisting heat and intense shear forces applied to the melt polymer compound during the calendering process. The results showed successful fabrication of the bio-composite sheets supported by the lowered melting temperature of the filled bio-composites, which is normally impossible through the utilization of common methods such as extrusion injection molding or

hot press due to the decreased wettability of natural fibers appearing at high filler loadings due to lack intense shear forces. The results further demonstrated the increased elastic tensile modulus response of the fabricated parts with the addition of filler whilst the strength experienced a decrease due to the formation of agglomeration and decreased wetting of kenaf fibers at higher filler content. The observed increased crystallization against the decrease in the density of the parts with kenaf wt% was correlated to the decrease in the toughness of the parts. The morphology and structural studies while supporting the changes in mechanical performance supported the high level of dispersion and distribution of the filler and kenaf/PLA interfacial interactions.

#### Acknowledge

We hereby acknowledge the Polymer and Nanocomposites Lab., Mechanical Eng. Dept., Isfahan University of Technology, Iran for providing equipment, materials, and scientific assistance.

## Nomenclature

$H_0$	Heat of fusion, $J/gr$
$Hm$	Heat of fusion of full crystalline polymer, $J/gr$
$K$	Crystal shape factor
$L$	Crystallite thickness, $nm$
$PI$	Peak intensity
$T_g$	Glass transition, $^{\circ}C$
$T_m$	Melt temperature, $^{\circ}C$
$\beta$	the full width at half maximum, $rad$
$X$	Crystallinity, $vol\%$

## References

- [1] A. Ashori, Wood-plastic composites as promising green-composites for automotive industries!, *Bioresour. Technol.*, 99(11) (2008) 4661-4667.
- [2] D.J. Gardner, Y. Han, L. Wang, Wood-Plastic Composite Technology, *Current Forestry Reports*, 1(3) (2015) 139-150.
- [3] G. Koronis, A. Silva, M. Fontul, Green composites: A review of adequate materials for automotive applications, *Compos. B. Eng.*, 44(1) (2013) 120-127.
- [4] E. Zini, M. Scandola, Green composites: an overview, *Polym. Compos.*, 32(12) (2011) 1905-1915.
- [5] R. Gunti, A. Ratna Prasad, A. Gupta, Mechanical and degradation properties of natural fiber-reinforced PLA composites: Jute, sisal, and elephant grass, *Polym. Compos.*, 39(4) (2018) 1125-1136.
- [6] R.B. Yusoff, H. Takagi, A.N. Nakagaito, Tensile and flexural properties of polylactic acid-based hybrid green composites reinforced by kenaf, bamboo and coir fibers, *Industrial Crops and Products*, 94 (2016) 562-573.
- [7] G.-L. Gavril, M. Wrona, A. Bertella, M. Świeca, M. Râpă, J. Salafranca, C. Nerín, Influence of medicinal and aromatic plants into risk assessment of a new bioactive packaging based on polylactic acid (PLA), *Food Chem. Toxicol.*, 132 (2019) 110662.
- [8] I.S. Tawakkal, M.J. Cran, S.W. Bigger, Effect of poly (lactic acid)/kenaf composites incorporated with thymol on the antimicrobial activity of processed meat, *Journal of Food Processing and Preservation*, 41(5) (2017) e13145.
- [9] P.K. Bajpai, I. Singh, J. Madaan, Development and characterization of PLA-based green composites: A review, *J. Thermoplast. Compos. Mater.*, 27(1) (2014) 52-81.
- [10] N. Sarifuddin, H. Ismail, Z. Ahmad, The Effect of Kenaf Core Fibre Loading on Properties of Low Density Polyethylene/Thermoplastic Sago Starch/Kenaf Core Fiber Composites, *Journal of Physical Science*, 24(2) (2013).
- [11] O. Seong, Han, M. Karevan, I.N. Sim, M. Bhuiyan, Y. Jang, J. Ghaffar, K. Kalaitzidou, Understanding the Reinforcing Mechanisms in Kenaf Fiber/PLA and Kenaf Fiber/PP Composites: A Comparative Study, *International Journal of Polymer Science*, 2012 (2012) 679252.
- [12] H. Anuar, A. Zuraida, J. Kovacs, T. Tabi, Improvement of mechanical properties of injection-molded polylactic acid-kenaf fiber biocomposite, *J. Thermoplast. Compos. Mater.*, 25(2) (2012) 153-164.
- [13] I. Tharazi, A. Sulong, N. Muhamad, C. Haron, D. Tholibon, N. Ismail, M.M. Radzi, Z. Razak, Optimization of hot press parameters on tensile strength for unidirectional long kenaf fiber reinforced polylactic-acid composite, *Procedia engineering*, 184 (2017) 478-485.
- [14] G. BEN, T. MATSUDA, Y. UENO, Development and mechanical properties of kenaf fibers green composites with pultrusion method, *Journal of the Japan Society for Composite Materials*, 36(2) (2010) 41-47.
- [15] G.S. Mann, L.P. Singh, P. Kumar, S. Singh, Green composites: A review of processing technologies and recent applications, *J. Thermoplast. Compos. Mater.*, 33(8) (2020) 1145-1171.
- [16] A.U. Birmin-Yauri, N.A. Ibrahim, N. Zainuddin, K. Abdan, Y.Y. Then, B.W. Chieng, Effect of maleic anhydride-modified poly (lactic acid) on the properties of its hybrid fiber biocomposites, *Polymers*, 9(5) (2017) 165.
- [17] I.S. Tawakkal, M.J. Cran, S.W. Bigger, Effect of kenaf fibre loading and thymol concentration on the mechanical and thermal properties of PLA/kenaf/thymol composites, *Industrial Crops and Products*, 61 (2014) 74-83.
- [18] N.I.A. Razak, N.A. Ibrahim, N. Zainuddin, M. Rayung, W.Z. Saad, The influence of chemical surface modification of kenaf fiber using hydrogen peroxide on the mechanical properties of biodegradable kenaf fiber/poly (lactic acid) composites, *Molecules*, 19(3) (2014) 2957-2968.
- [19] N. Graupner, J. Rößler, G. Ziegmann, J. Müssig, Fibre/matrix adhesion of cellulose fibres in PLA, PP and MAPP: a critical review of pull-out test, microbond test and single fibre fragmentation test results, *Compos. - A: Appl. Sci. Manuf.*, 63 (2014) 133-148.
- [20] M. Nematollahi, M. Karevan, P. Mosaddegh, M. Farzin, Morphology, thermal and mechanical properties of extruded injection molded kenaf fiber reinforced polypropylene composites, *Materials Research Express*, 6(9) (2019) 095409.
- [21] M. Nematollahi, M. Karevan, M. Fallah, M. Farzin, Experimental and Numerical Study of the Critical Length of Short Kenaf Fiber Reinforced Polypropylene Composites, *Fibers and Polymers*, 21(4) (2020) 821-828.
- [22] T.-J. Chung, J.-W. Park, H.-J. Lee, H.-J. Kwon, H.-J. Kim, Y.-K. Lee, W. Tai Yin Tze, The improvement of mechanical properties, thermal stability, and water absorption resistance of an eco-friendly PLA/kenaf biocomposite using acetylation, *Applied Sciences*, 8(3) (2018) 376.
- [23] S. Jia, D. Yu, Y. Zhu, Z. Wang, L. Chen, L. Fu, Morphology, crystallization and thermal behaviors of PLA-based composites: wonderful effects of hybrid GO/PEG via dynamic impregnating, *Polymers*, 9(10) (2017) 528.

- [24] A. Gao, Y. Zhao, Q. Yang, Y. Fu, L. Xue, Facile preparation of patterned petal-like PLA surfaces with tunable water micro-droplet adhesion properties based on stereo-complex co-crystallization from non-solvent induced phase separation processes, *Journal of Materials Chemistry A*, 4(31) (2016) 12058-12064.
- [25] Z. Abdul Hamid, Surface Modification of Poly (lactic acid) (PLA) via Alkaline Hydrolysis Degradation, *Advanced Materials Research*, 970 (2014) 324-327.
- [26] J.-M. Park, J.-Y. Choi, Z.-J. Wang, D.-J. Kwon, P.-S. Shin, S.-O. Moon, K.L. DeVries, Comparison of mechanical and interfacial properties of kenaf fiber before and after rice-washed water treatment, *Compos. B. Eng.*, 83 (2015) 21-26.
- [27] M.S. Huda, L.T. Drzal, A.K. Mohanty, M. Misra, Effect of fiber surface-treatments on the properties of laminated biocomposites from poly (lactic acid)(PLA) and kenaf fibers, *Compos. Sci. Technol.*, 68(2) (2008) 424-432.
- [28] H. Anuar, A. Zuraida, Thermal properties of injection moulded polylactic acid-kenaf fibre biocomposite, *Malaysian Polymer J*, 6(1) (2011) 51-57.
- [29] G. Papageorgiou, D. Achilias, S. Nanaki, T. Beslikas, D. Bikiaris, PLA nanocomposites: Effect of filler type on non-isothermal crystallization, *Thermochim. Acta*, 511(1-2) (2010) 129-139.
- [30] D. Wu, L. Wu, L. Wu, B. Xu, Y. Zhang, M. Zhang, Nonisothermal cold crystallization behavior and kinetics of polylactide/clay nanocomposites, *J. Polym. Sci., Part B: Polym. Phys.*, 45(9) (2007) 1100-1113.
- [31] P.-Y. Chen, H.-Y. Lian, Y.-F. Shih, S.-M. Chen-Wei, R.-J. Jeng, Preparation, characterization and crystallization kinetics of Kenaf fiber/multi-walled carbon nanotube/poly(lactic acid) (PLA) green composites, *Mater. Chem. Phys.*, 196 (2017) 249-255.
- [32] S.O. Han, M. Karevan, I.N. Sim, M.A. Bhuiyan, Y.H. Jang, J. Ghaffar, K. Kalaitzidou, Understanding the reinforcing mechanisms in kenaf fiber/PLA and kenaf fiber/PP composites: A comparative study, *International Journal of Polymer Science*, 2012 (2012).
- [33] R. Qiao, H. Deng, K.W. Putz, L.C. Brinson, Effect of particle agglomeration and interphase on the glass transition temperature of polymer nanocomposites, *J. Polym. Sci., Part B: Polym. Phys.*, 49(10) (2011) 740-748.
- [34] J. Seiler, J. Kindersberger, Insight into the interphase in polymer nanocomposites, *IEEE Trans Dielectr Electr Insul*, 21(2) (2014) 537-547.
- [35] O.K.C. Tsui, T.P. Russell, C.J. Hawker, Effect of interfacial interactions on the glass transition of polymer thin films, *Macromolecules*, 34(16) (2001) 5535-5539.
- [36] W. Zhao, Y. Su, X. Gao, J. Xu, D. Wang, Interfacial effect on confined crystallization of poly (ethylene oxide)/silica composites, *J. Polym. Sci., Part B: Polym. Phys.*, 54(3) (2016) 414-423.
- [37] Z. Tang, C. Zhang, X. Liu, J. Zhu, The crystallization behavior and mechanical properties of polylactic acid in the presence of a crystal nucleating agent, *J. Appl. Polym. Sci.*, 125(2) (2012) 1108-1115.
- [38] J. Feng, S.R. Venna, D.P. Hopkinson, Interactions at the interface of polymer matrix-filler particle composites, *Polymer*, 103 (2016) 189-195.
- [39] F. Jones, A review of interphase formation and design in fibre-reinforced composites, *J. Adhes. Sci. Technol.*, 24(1) (2010) 171-202.
- [40] S.H. Ghaffar, O.A. Madyan, M. Fan, J. Corker, The influence of additives on the interfacial bonding mechanisms between natural fibre and biopolymer composites, *Macromolecular Research*, 26(10) (2018) 851-863.
- [41] A. Hassan, M.M. Isa, Z.M. Ishak, N. Ishak, N.A. Rahman, F.M. Salleh, Characterization of sodium hydroxide-treated kenaf fibres for biodegradable composite application, *High Perform. Polym.*, 30(8) (2018) 890-899.
- [42] N. Saba, M. Paridah, M. Jawaid, Mechanical properties of kenaf fibre reinforced polymer composite: A review, *Construction and Building materials*, 76 (2015) 87-96.
- [43] Y. Zare, K.Y. Rhee, D. Hui, Influences of nanoparticles aggregation/agglomeration on the interfacial/interphase and tensile properties of nanocomposites, *Compos. B. Eng.*, 122 (2017) 41-46.

#### HOW TO CITE THIS ARTICLE

M. Karevan, *Poly(lactic Acid) /High-Ratio Natural Kenaf Fiber Biocomposite Sheets Processed by Calendering Melt Mixing Technique*, *AUT J. Mech Eng.*, 6(3) (2022) 387-400.

DOI: [10.22060/ajme.2022.20621.6010](https://doi.org/10.22060/ajme.2022.20621.6010)

